16TH EUROPEAN CONFERENCE ON EARTHQUAKE ENGINEERING THESSALONIKI 18 - 21 JUNE 2018

OPTIMISING RESOLUTION AND IMPROVEMENT STRATEGIES FOR EMERGING GEODATABASES IN DEVELOPING COUNTRIES

Charlotte E. L. GILDER[1], Raffaele DE RISI[2], Flavia DE LUCA[3], Paul J. VARDANEGA[4], Elizabeth A. HOLCOMBE[5], Peyman AYOUBI[6], Domniki ASIMAKI[7], Rama Mohan POKHREL[8], Anastasios SEXTOS[9,10]

ABSTRACT

Geotechnical and geological data are needed for the seismic hazard assessments that inform earthquake risk management and resilient engineering design. This paper reviews information typical of that available in developing countries for the definition of the shear wave velocity in the first 30 meters of soil (V_{S30}). This paper aims to determine optimal resolutions for different data sources in relation to the definition of V_{S30} maps and the identification of an optimal strategy for localisation of new site investigations (i.e., new boreholes). The context of developing countries, being characterised by endemic lack of high-quality archived data and lack of systematic financial sources, makes the scope of the study challenging and different from the geological and geotechnical approaches typically used in developed countries. Within this context, the auxiliary employment of empirical correlations for the evaluation of V_{S30} is also discussed as a means of defining cost-effective investigation strategies for developing countries. The Kathmandu Basin in Nepal is used as a representative case study. Preliminary data collected within the University of Bristol led project SAFER - *Seismic Safety and Resilience of Schools in Nepal* - are critically analysed to the aim of identifying (i) the critical resolution for geodatabase layers (e.g., the digital elevation model) and (ii) the best location for new borehole tests aimed at improving the quality of the V_{S30} model for the Basin. The approach outlined for Nepal is applicable to other seismic prone areas in the developing world.

Keywords: Kathmandu Basin; shear-wave velocity; regression analysis; digital elevation model; kriging.

1. INTRODUCTION

Local geological and topography conditions play a crucial role together with magnitude and distance into the determination of intensity of ground motion. The geological structure of the region is important information, but the local site condition is known to have an even more relevant role on amplification and damage (Seed and Idriss 1969).

The parameter used in design codes such as Eurocode 8 (CEN 2004) and Ground Motion Prediction Equations (GMPEs) for soil classification is the average of shear-wave velocity from the surface to 30m depth (V_{S30}). This parameter can be estimated through various measuring techniques active or passive (Foti et al. 2017) or using indirect correlations with geotechnical parameters such as the Standard Penetration Test (SPT-N) (e.g., Ohta and Goto 1978; Jafari et al. 2002; Dikmen 2009; Gautam 2017).

[1]PhD student, Civil Engineering, University of Bristol, Bristol, UK, charlotte.gilder@bristol.ac.uk
[2]Research Associate, Civil Engineering, University of Bristol, Bristol, UK, raffaele.derisi@bristol.ac.uk
[3]Lecturer, Civil Engineering, University of Bristol, Bristol, UK, flavia.deluca@bristol.ac.uk
[4]Lecturer, Civil Engineering, University of Bristol, Bristol, UK, p.j.vardanega@bristol.ac.uk
[5]Senior Lecturer, Civil Engineering, University of Bristol, Bristol, UK, liz.holcombe@bristol.ac.uk
[6]PhD student, Mechanical and Civil Engineering, Caltech, Pasadena, USA, ayoubi@caltech.edu
[7]Professor, Mechanical and Civil Engineering, Caltech, Pasadena, USA, domniki@caltech.edu
[8]CEO, Earth Investigation and Solution Nepal Pvt. Ltd., Kathmandu, Nepal, pokhrelmohan@gmail.com
[9]Reader, Civil Engineering, University of Bristol, Bristol, UK, a.sextos@bristol.ac.uk
[10]Associate Professor, Civil Engineering, Aristotle University, Thessaloniki, Greece, asextos@civil.auth.gr

A preliminary estimation of soil classification (corresponding to a range of V_{S30}) can be obtained from 'expert opinion' in combination with geological maps of shallower deposits (e.g., Di Capua et al. 2011). V_{S30} can be estimated also from correlation with slope obtained from Digital Elevation Models (DEM) in the following, (Wald and Allen 2007) and it is the basic standard used by United States Geological Survey (USGS), for shake maps implemented in the software package ShakeMap® developed by the USGS Earthquake Hazards Program (Wald et al. 2006). The V_{S30} parameter is used by engineers as a way of characterising an areas susceptibility to earthquake hazard and can be calculated according to Eurocode 8 (CEN 2004, clause 3.1.2). The parameter is also used in building code in the United States Standard ASCE 7-10 (ASCE 2010). V_{S30} is not the only parameter suitable and used to define soil amplification effects, and many authors in recent years have emphasised how, in some specific conditions like basins (e.g., Stewart et al. 2003; Paudyal et al. 2013), it is not strongly correlated with site amplification (e.g., Castellaro et al. 2008; Gallipoli and Mucciarelli 2009; Lee and Trifunac 2010; Luzi et al. 2011). Site response is characterised by the velocity contrast between two successive layers of soil, and the V_{S30} calculation, is simplifying this relationship to an average value over the first 30m of soil encountered. The use of this assumption in areas displaying high lateral variability and where deeper soils are characterising the response, can lead to unrealistic predictions of the soils stiffness profile and therefore its response to earthquake hazard. The selection of the best parameter or set of parameters to describe soil amplification becomes even more challenging in the context of developing countries. Here, an often systematic lack of data can significantly limit the opportunities to obtain a satisfactory dataset for accurate soil amplification definition, especially in complex contexts like basins. This study presents an investigation of methods to refine site amplification definition in the context of a representative developing country.

In particular, a case study of the Kathmandu Basin in the Federal Democratic Republic of Nepal is presented. The Basin lies on the Kathmandu Nappe (Paudyal et al. 2013); one of several intermontane basins that have formed along the lesser Himalaya (Sakai et al. 2002). This area experienced significant amplification during the M_w 7.8 Gorkha earthquake that struck Nepal on the 25th of April 2015, causing significant damage in some specific areas of the Kathmandu Basin (e.g., Goda et al. 2015; Ohsumi et al. 2016). Such amplification was retrieved from the single record available right after the earthquake at KATNP accelerometric station managed by USGS, where the estimated peak ground accelerations range between 150-170 cm/s² for the mainshock, predicted through inspection of the time-history data (Goda et al. 2015). As a result of this, more recently, a series of microtremor studies (e.g., Tallett-Williams et al. 2016; Molnar et al. 2017; Poovarodom et al. 2017) and simulations of the amplification effect of the Basin (e.g., Asimaki et al. 2017) have been reported. These investigations have built upon studies published before the occurrence of the 2015 earthquake during which a significant amount of test data was collected (see Piya 2004).

The two research questions preliminary addressed herein are whether: (i) an increase in the resolution of the DEM can improve the accuracy of V_{S30} estimation on the basis of slope; and (ii) if a kriging method (e.g., Pokhrel et al. 2013) coupled either with available V_{S30} measurements or bespoke indirect correlations can guide the identification of further locations for boreholes.

2. DIRECT AND INDIRECT DATA FOR SHEAR WAVE VELOCITY

2.1 Seismic acquisition methods

Classification of the near surface shear-wave V_{S30} at a site can be approximated from a variety of seismic acquisition techniques. According to Eurocode 8 (CEN 2004, clause 3.1.2), V_{S30} is defined as shown in Equation 1, where h_i and v_i denote the thickness (in metres) and shear-wave velocity of the i-th formation or layer, in a total of N layers, existing in the top 30 m.

$$V_{S30} = \frac{30}{\sum_{i=1,N} \frac{h_i}{v_i}} \tag{1}$$

The shear-wave velocity can be approximated by undertaking cross-hole or downhole seismic methods, Seismic Cone Penetration Tests (SCPT's) (Wair et al. 2012), or by design of a detector array for which both source and receivers are arranged at the ground surface (Andrus et al. 2004). The quality of data acquired for V_{S30} measurement is affected by the technique used. When seismic acquisition techniques are performed in developing countries, these tests are often not carried out due to the costs associated with procurement of the necessary technical equipment and the complex data processing. Here, non-intrusive surface wave methods are an attractive alternative. A recent review by Foti et al. (2017), described the findings of an EU funded project aiming to provide a practical approach targeted at non-expert users in such a scenario. The work describes optimised acquisition layouts during the Spectral Analysis of Surface Wave test (SASW) or by Multichannel Analysis of Surface Waves (MASW) (Park et al. 1999). According to Foti et al. (2017), passive type methodologies without the use of an artificial seismic source, can be a cost-effective alternative. The shear wave velocity profile is obtained by achieving a best fit between the experimental dispersion curve, obtained from processing of the field data, and a theoretical dispersion curve produced from model parameters (Foti et al. 2017). This process is not without error as, "the number of layers must be fixed carefully in order to avoid over-parametrization" (Foti et al. 2017) (e.g., stratigraphy or any other borehole measurements), however, where further information cannot be obtained, the process is useful.

2.2 Empirical correlations

In many areas of the world, including Kathmandu, it is now standard practice to perform geotechnical observations (i.e. SPT-N) where a reasonably important building is to be constructed. However, for the case of the Kathmandu Basin there is a lack of information on the basins sediments spatial variation (Paudyal et al. 2013). As V_S is related to the small strain shear modulus (G_{max}), measurements of shear wave velocity when coupled with engineering parameters can be correlated empirically. Standard Penetration Tests (SPT's) are undertaken at increment within boreholes, for which a blow count (SPT-N) is derived based on the dropping of a known weight, over a specified length of penetration. This parameter provides information on the geotechnical engineering properties of the soil and is used as an indication of strength for the design of foundations. Various authors have explored this parameter, along with other geotechnical properties with V_{S30} (e.g., Anbazhagan et al. 2012). In many cases, these attempts provide bespoke correlations which account for the material type and the stratigraphic relationships specific to the region studied (e.g., Pitilakis et al. 1999; Fabbrocino et al. 2015). Among the regional correlations available in literature, Gautam (2017) reported a correlation between uncorrected SPT-N and shear wave velocity for the Kathmandu Valley. These correlations should be used with caution and suggested processing techniques are described in the literature, which present statistical methods to better refine estimates (Brandenberg et al. 2010; Aung and Leong 2015). Where data is lacking in Kathmandu these relationships will form the basis of this research, where seismically derived V_{S30} is absent, to present a method of highlighting those areas which are most vulnerable, or 'data poor' to present existing information in a new liquefaction hazard map and inform further study.

3. AVAILABLE DATA FOR KATHMANDU BASIN

3.1 Basin Characteristics

The Kathmandu Basin in Central Nepal is characterised by Pliocene and early Pleistocene lake deposits overlain by younger silty Quaternary deposits (Dill 2006). The Engineering and Environmental Geological Map of the Kathmandu Valley (Shrestha et al. 1998) shows a reasonable overview of the underlying geology. The deposits of the historic intermontane lake, extend to depths of approximately 400m to 600m below the city of Kathmandu. A 284m-deep borehole reveals a sequence of black organic mud known as the Kalimati Clay, which is overlain by younger fluvio-deltaic sediments Gokarna, Thimi and Patan formations (Fujii and Sakai 2002). The wider area is more famously known to comprise a thrust zone, due to the Himalayan orogeny, which has formed successive metamorphic sequences (Guillot 1999) that underlie the Basin sediments. The research team of the EPSRC funded project Seismic Safety and Resilience of Schools in Nepal (SAFER) (Grant code: EP/P028926/1) has access to

a database of borehole records from the Kathmandu Valley, sourced from various consultants and historic records. The records include some detailed records (including *in situ* SPT testing or laboratory data), whereas the majority indicate only basic log information and locations. Six locations have corresponding P-S logging, where shear wave (V_S) values are provided relating to depth derived from downhole methods. These boreholes are listed in Table 1 and the locations are shown in Figure 1(a).

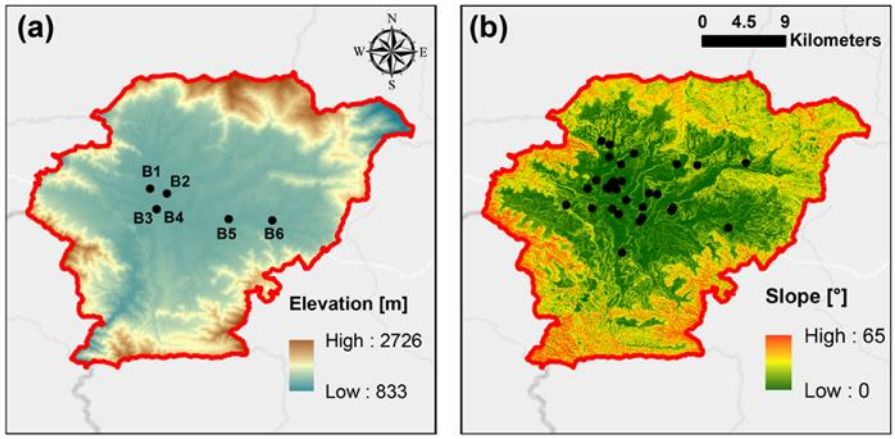

Figure 1. (a) 10-m resolution digitalized elevation model and (b) slope map. Black dots represent the (a) locations of the V_{S30} and (b) SPT measurements.

The borehole data has indicated the Kathmandu soils comprise of a mixture of silty clay, clayey silt, sandy clay and occasional silty sand. Out of 76 particle size distribution tests 73 samples are comprising either a silty clay of clayey silt. Figure 2 shows that the plasticity of these soils varies from low to very high. The data plots mainly below the A-line which indicates the soils are generally silty. Figure 2 gives an overview of the available soil classification data from Kathmandu but does not distinguish between different geological deposits.

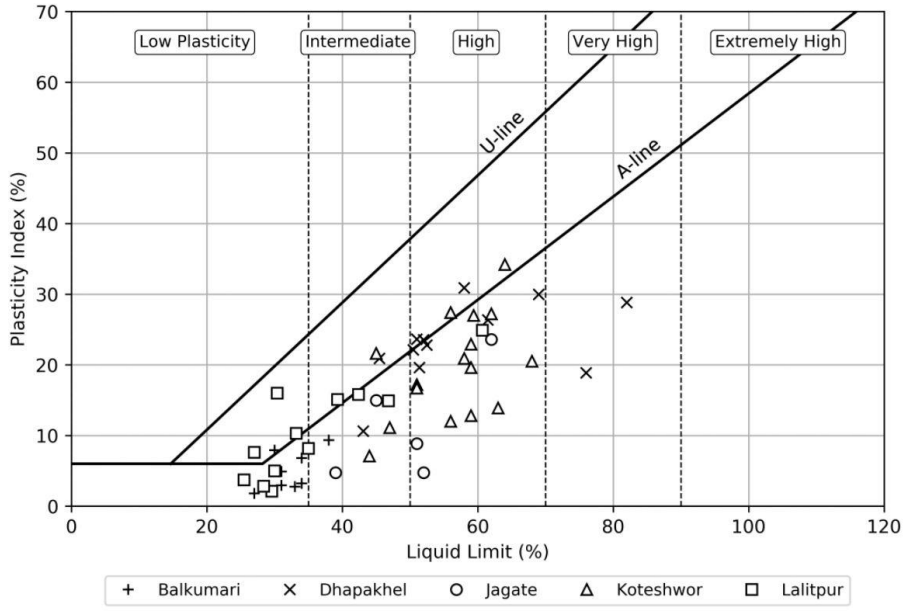

Figure 2. Classification of the Kathmandu soil data. Chart layout based on Casagrande (1947), Howard (1984) and BS 5930 (clause 33.4.4.4) (BSI 2015).

3.2 SPT-N with V_{S30} Correlation

As described in section 2, the preferred method of deriving V_{S30} is based on site specific information and good quality seismic acquisition. In this study, where there is a lack of detailed information, to build upon the low number of measured V_S values, SPT-N values were extracted from the borehole records to use within the equation presented by Gautam (2017). Figure 3 shows a plot of the measured V_S data against SPT-N values from the six sites referenced in Table 1. The power regression analysis reported in Gautam (2017). This regression model was developed from a database of 500 pairs of SPT-N values and measured VS from the Kathmandu Basin, and represents a correlation developed for all soil types.

Table 1. Site Referencing Information

BH ID	Location	Project	Latitude	Longitude
BH-1	Ranjana	New Road, Fire Brigade Compound	27.70353	85.30879
BH-2	Singha Durbar	Northern Periphery Road, Singh Durbar	27.69878	85.32511
BH-3	Bakhundol	Royal Norwegian Embassy	27.68335	85.31509
BH-4	Bakhundol	Royal Norwegian Embassy	27.68320	85.31533
BH-5	Thimi	Near Altech (P) Ltd, Arniko Highway	27.67355	85.38568
BH-6	Bhaktapur	Durbar Square, Bhaktapur	27.67216	85.42822

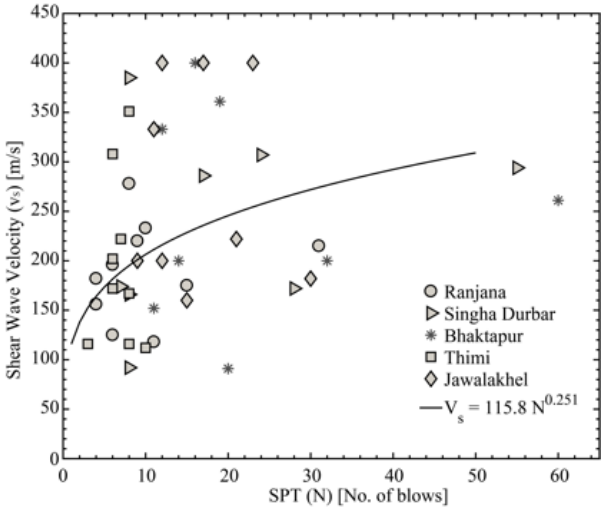

Figure 3. Comparison of measured shear wave velocity (V_S) with uncorrected SPT-N values at five sites across Kathmandu. The trendline shown is from the regression study performed by Gautam (2017) on a different data-set and is described by the equation $V_S = 115.8N^{0.251}$ ($R^2 = 0.623$).

Where SPT-N data is available in the first 30m, the velocities were calculated and used to determine an estimated V_{S30} for that location using the correlation. Where boreholes were less than 30m in depth, SPT-N records were taken, and a correction was applied according to Boore (2004) where boreholes extended to at least 10m, for which application of the correction can begin. The locations where estimation of V_{S30} was carried out are shown on Figure 1(b). A total of 31 additional locations have been made available to the SAFER project team for analysis based on this method.

As discussed in Section 2, it is acknowledged that other correlations for V_{S30} to SPT-N values exist in the literature (Jafari et al. 2002; Dikmen 2009). For example, Ohta and Goto (1978) found greatest correlation to V_S when accounting for SPT-N, depth, geological epoch and soil type. Other correlations for geotechnical parameters including PI and undrained shear strength (Wair et al. 2012). However, all other correlations are describing characteristics which are not unique to the Kathmandu Basin, therefore as a preliminary assessment, the location-specific correlation has been used. Currently, only SPT-N

values have been extracted for correlation. It is expected that further work with the current dataset to incorporate age scaling factors, an adjustment for material type and overburden corrections, could be incorporated into the predictions (e.g., Ohta and Goto 1978) with the intent to improve upon the presented methodology for estimating V_{S30} in developed countries.

4. CHALLENGES AND RESULTS

The main problem in developing countries is the lack or the total absence of geological and geotechnical data for seismic hazard assessment (Anttila-Hughes et al. 2015). For the purposes of seismic microzonation of large geographical areas, a large number of advanced geotechnical tests (e.g., MASW) may be needed. Such tests are usually prohibitively expensive which precludes their application in developing countries. This raises three significant practical challenges. First, are there freely available data that can be used in absence of detailed rigorous tests? Second, is there a way to optimise the number of tests on a geographical area to reduce the cost of the investigation? Third, can low-cost tests be used as an alternative to more expensive ones using empirical correlations transforming basic geotechnical parameters to more sophisticated ones? In the following these three questions are addressed referring to the data available for the case of Kathmandu Basin described in the previous section.

4.1 Topographic slope as a proxy for V_{S30}

Wald and Allen (2007) propose a methodology to estimate the shear wave velocity as function of slope. A regression function was applied to create a global database with a resolution of 30-arcsec (about 900 m). Figure 4(a) shows the V_{S30} map obtained from the database information provided for the Kathmandu Valley. Given the availability of a higher resolution DEM (i.e., 10m), the same correlation was implemented to establish if a refined version improves the estimation of V_{S30}. Therefore, applying the same Wald and Allen's regression function an independent V_{S30} map (Figure 4b) was obtained. Comparing the two maps in Figure 4, it is possible to conclude that the trend is similar (i.e., high values for the mountains and lower values for the approximately level basin depression), but the distribution of values is significantly different.

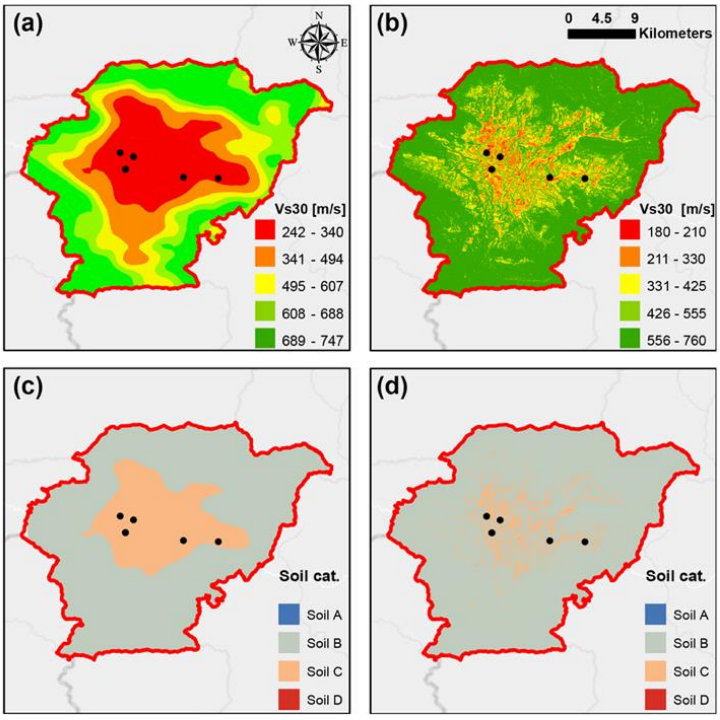

Figure 4. (a) USGS and (b) 10m-DEM-based V_{S30} maps; soil categorization according to EC8 (CEN 2004) based on (c) USGS and (d) 10m-DEM-based V_{S30} maps, respectively.

An additional investigation inspecting the effect of the refined DEM on the overall Eurocode 8 soil classification (where soil A is rock and the other soils up to E are progressively softer), on Figure 4 Soils A – D are specified, see CEN 2004, clause 3.1.2 for details of further categories. Adopting the classification proposed by Eurocode 8 (CEN 2004), a significant mismatching is found when using the high-resolution DEM, leading to a considerable overestimation of shear wave velocities, and therefore an underestimation of the expected seismic intensities. Figure 5 shows the comparison of the V_{S30} maps with the available borehole data. Figure 5 shows that all the 10m-DEM-based values tend to overestimate the measured V_{S30} even when an averaging of the values is made over a radius (R). Even artificially varying the resolution (by averaging data within a radius varying between 10 m to 1000 m) does not bring any benefit in terms of prediction.
The USGS data, which is the coarser in spatial terms (represented as cyan dots in Figure 5), tend to give a better prediction than any of the estimations carried out with the 10m-DEM. This result confirms that observed by Allen and Wald (2009), showing "... little to no improvement over lower-resolution topography when compared to V_{S30} measurements ... [and therefore] some topographic smoothing may provide more stable V_{S30} estimates" (Allen and Wald, 2009). An alternative is the calibration of bespoke models for slope-DEM regression as it has been recently proposed by Stewart et al. (2014).

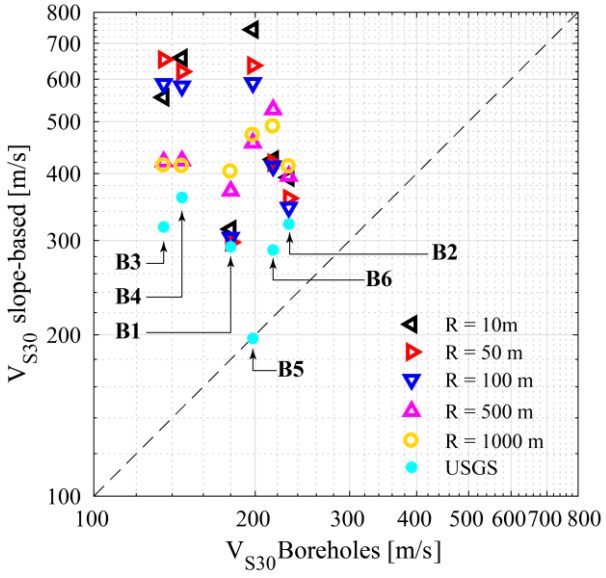

Figure 5. Comparison of V_{S30} values obtained from filed data and DEM-based V_{S30}

4.2 Kriging interpolation with available direct and indirect data

To obtain V_{S30} maps that cover a wider part of the case study area, data coming from field tests can be used in a geostatistical framework through the adoption of a kriging analysis (Stein 2012). "The kriging method is widely used in GIS to obtain spatial distribution of geographical information. Kriging is one of the most exact and powerful interpolation schemes in geostatistics" (Pokhrel et al. 2013). Using the V_{S30} values available in Kathmandu kriging was applied in this work. Figure 6a shows the results of kriging in terms of predicted values of V_{S30} in between the measured. In Figure 6b, the same kriging is done using the results from the indirect values inferred from the empirical correlation reported in Gautam (2017). Figures 6c and 6d show the standard error associated with the geostatistical analyses in Figures 6a and 6b respectively.
The error is at a minimum at each borehole (measurement) location and increases with increasing distance from these measurements. Examination of the error map is possible to identify potential locations for new field investigations. From a purely hazard-focused standpoint, these locations would be selected by trying to reduce the maximum error (i.e., the red area in Figures 6c and 6d). However, to account for overall risk, additional constraints could be considered such as the location, or exposure, of at-risk elements (such as people, structures and infrastructure) and their vulnerability to earthquake damage. In a wide-area analysis, it is important to have proper characterisation of the hazard in the areas

of maximum exposure and vulnerability. Therefore, the location of the future detailed geotechnical investigations should aim to achieve the best possible trade-off between the error limitation (in a geo-statistical sense) and the necessity of refined geo-characterisation in areas where the exposure and vulnerability is highest. For example, in the case proposed in Figure 6c, a suitable location for a new geotechnical investigation would be close to the ring road (within the orange area in Figure 6c), comprising the area with highest uncertainty and coinciding with a densely populated, and consequently highly exposed and vulnerable, zone. The comparison of the rectangular areas shown in Figure 6a and 6b, highlights that with adoption of the empirical relationship presented by Gautam (2017) and discussed in section 3, relating SPT-N to V_{S30} for Kathmandu, leads to an overestimation of the shear wave velocity. Therefore, it is highly desirable to improve the regional empirical formulation by including additional variables or considering a different regression strategy, as explained in section 3.2.

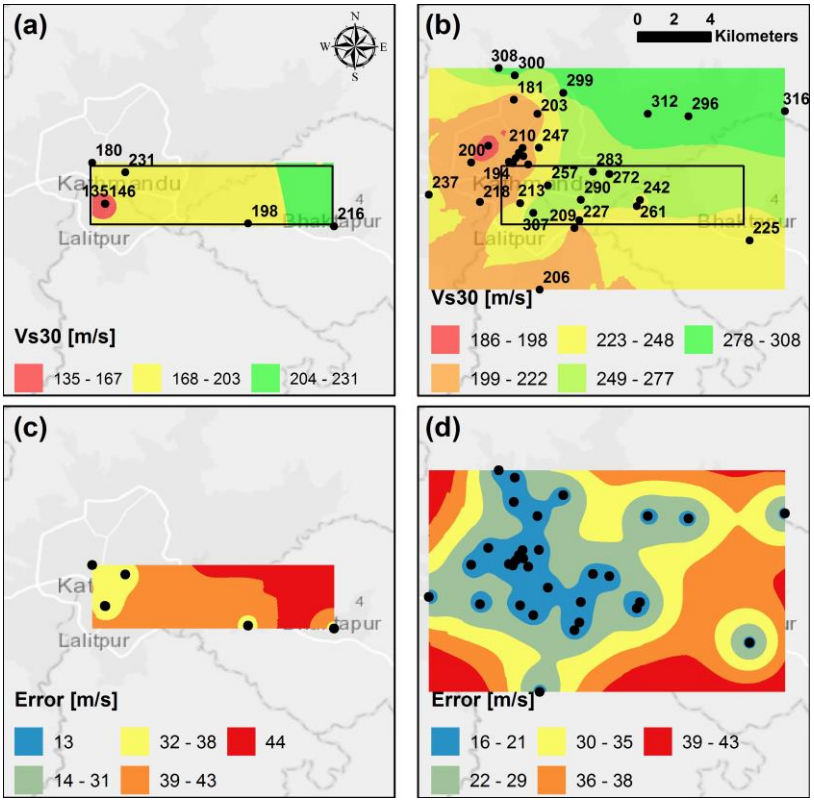

Figure 6. Kriging based on (a) measured V_{S30} and on (b) V_{S30} obtained from empirical correlation with SPT-N. Standard error based on (c) measured and (d) empirically inferred V_{S30}.

4.3 Numerical simulation of Kathmandu valley during the mainshock of 2015 Gorkha earthquake

A simple numerical experiment to demonstrate the relative role of source, path (basin) and site (shallow crustal) effects on the ground surface response recorded during the 2015 Gorkha mainshock was carried out. For this experiment, site-specific velocity profiles at two strong motion stations (PTN and TVU) are used, on sediments reported by Bijukchhen et al. (2017). An averaged profile was extrapolated to the sediment-basement rock interface to approximate the stratigraphy of 2D simulations, an idealised geometry of the basin adopted from Piya (2004) and the rock outcrop ground motion recording of the Mw 7.8 mainshock at station KTP. With the above information, 1D nonlinear site response analyses were performed at the two stations using the computer code SEISMOSOIL (Shi and Asimaki 2017) with the KTP recording as rock outcrop input. In addition, 2D linear viscoelastic analyses were performed using the computer code OPENSEES (McKenna et al. 2000), available at http://opensees.berkeley.edu/, with the KTP recording deconvolved at depth below the basin as incident plane wave, and the averaged velocity profile as the horizontally stratified sediments of the basin (see Ayoubi et al. 2018 for further information). The results are shown in Figure 7 and can be summarised as follows:

(a) Station PTN is located close to the middle of the basin, where the wave propagation conditions could be assumed to be 1D. This is observed in the comparison of response spectra of Figure 7, where the simulated 1D nonlinear ground response compares very well to the recorded ground shaking in the period range 1-5 sec. 2D simulations perform poorly, most likely because nonlinear effects dominate the ground motion at this station compared to the focusing and diffraction effects that 2D viscoelastic analyses can capture. As anticipated, the situation is reversed in the longer period range, where the surface waves originating at the basin edges dominate the response, and since nonlinear effects are not as prominent, 1D simulations does not sufficiently capture the physics of long period ground motion.
(b) Station TVU is located closer to the basin edge, where the response is expected to be dominated by 2D nonlinear effects through the entire period range. The period range 1-5 seconds is underestimated by both 1D and 2D analyses; note that the former does not capture basin edge focusing effects and the latter does not include nonlinear response or a high-resolution profile that can capture wave propagation effects of high frequencies. The comparison between 2D simulations and recordings improves for longer periods, since again surface waves from the basin edges dominate the ground motion in these periods, and 1D simulations also do not sufficiently capture the physics of these motions.

The source physics, which included a plane rupture practically parallel to the surface, determined the waveform characteristics of the propagating motions, over the entire spectrum and across the basin. Considering that the rupture propagated from west to east (from TVU to PTN), it is possible that directivity effects played a role in the ground shaking recorded at both stations; this could be why recorded components were underestimated by the 2D simulations in the long period range.
Lastly, frequencies higher than 1Hz (not shown here), where higher resolution vertical and lateral material heterogeneities and high frequency source energy radiation determine the response, were very poorly captured. The risk for low rise structures in developing counties like Nepal is predominantly affected by such high frequency components. In addition to this, the lack of high frequency ground motion records in the region. Therefore, developing 2D/3D high fidelity geotechnical characterisation models coupled with realistic source models through physics-based earthquake simulations is an appropriate way to characterise regional seismic risk, in future work.

5. CONCLUSIONS

A preliminary investigation on the strategies for improving accuracy of geodatabases and for rationalising geotechnical investigations in the context of developing countries is discussed. The specific questions addressed are whether: (i) an increase in the resolution of the DEM can improve the accuracy of V_{S30} estimation on the basis of slope; and (ii) if a kriging method coupled either with available V_{S30} measurements or bespoke indirect correlations can guide the identification of location of further boreholes. Lastly, a discussion of the current knowledge of the basins stratigraphy and response to ground motion, based on microtremor observations is presented.
The increased resolution of the DEM does not benefit the accuracy of V_{S30} and this result is aligned with previous studies available in literature. The general trend observed is a systematic overestimation of the V_{S30} as a result of the increased DEM resolution.
The employment of kriging as a technique for the smart identification of new investigations can provide some useful guidance. Future geotechnical tests can be targeted in the areas where the standard error from the kriging procedure is higher. This approach can be coupled with an assessment of the exposure and vulnerability characteristics of the area to assist with the identification of suitable locations for investigation. A further application of the kriging technique was attempted using a distribution of V_{S30} parameters resulting from predictions using a bespoke empirical correlation model for the Kathmandu Basin. In this case the V_{S30} was again overestimated and when the kriging was reapplied to the larger dataset, did not lead to a practical suggestion for the location of new investigations. Currently, the approximation of V_{S30} is based on the single correlation which is overestimating the measured values. The validity of this model can only be tested further by comparison with further seismic data or analytical ground surface response analyses acknowledging the role of source, basin and site effects.

However, with rigorous statistical analysis and further site investigation, the correlation may be improved to better inform analysis of the variation of amplifying effects and therefore regions of greater vulnerability across the Kathmandu Basin.

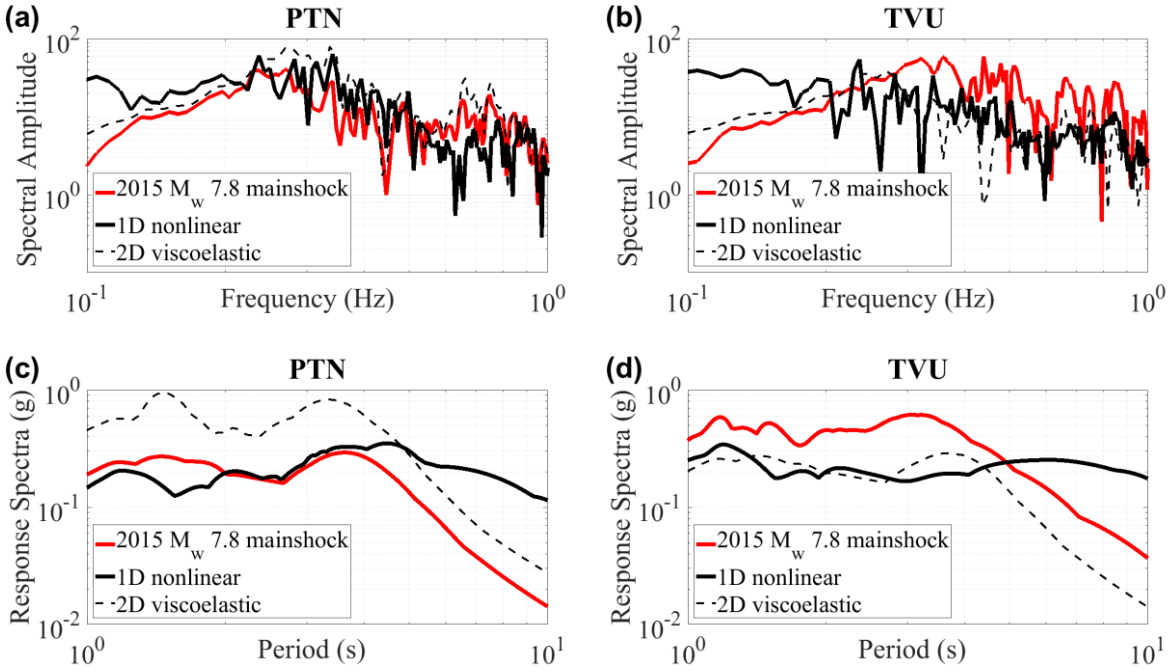

Figure 7. Acceleration spectral amplitudes for recording station (a) PTN and (b) TVU in the Kathmandu basin and acceleration response spectra for station (c) PTN and (d) TVU showing the site amplification response as recorded (red solid line) compared with 1D (black solid line) and 2D (black dashed line) analyses.

6. ACKNOWLEDGMENTS

This work was funded by the Engineering and Physical Science Research Council (EPSRC) under the project "Seismic Safety and Resilience of Schools in Nepal" SAFER (EP/P028926/1). Supporting data for this study are from third party sources. All data produced in this study are available upon request to bona fide researchers.

7. REFERENCES

Allen TI, Wald DJ (2009). On the Use of High-Resolution Topographic Data as a Proxy for Seismic Site Conditions (V_{S30}). *Bulletin of the Seismological Society of America*, 99(2A): 935-943.

Anbazhagan P, Parihar A, Rashmi HN (2012). Review of correlations between SPT N and shear modulus: A new correlation applicable to any region. *Soil Dynamics and Earthquake Engineering*, 36: 52-69.

Andrus D, Stokoe K, Juang H (2004). Guide for Shear-Wave-Based Liquefaction Potential Evaluation. *Earthquake Spectra*, 20(2): 285-308.

Anttila-Hughes J, Dumas, M, Jones L, Pestre G, Qiu Y, Levy M, et al. (2015). Big data for climate change and disaster resilience: Realising the benefits for developing countries. *Synthesis Report*. Data-Pop Alliance, 60 pp.

ASCE (2010). Minimum design loads for buildings and other structures. *Standard ASCE 7-10*, Reston, VA.

Asimaki D, Mohammadi K, Mason HB, Adams RK, Rajaure S, Khadka D (2017). Observations and Simulations of Basin Effects in the Kathmandu Valley During the 2015 Gorkha Earthquake sequence. *Earthquake Spectra*, 33(S1): S35-S53.

Aung AMW, Leong EC (2015). Application of a weighted average velocity (WAVe) method to determine $V_{S,30}$. *Soils and Foundations*, 55(3): 548-558.

Ayoubi P, Asimaki D, Mohammadi K (2018). Basin effects in strong ground motion: A case study from the 2015 Gorkha, Nepal earthquake. Paper to be presented at: *Geotechnical Earthquake Engineering and Soil Dynamics V*, June 10-13, 2018, Austin, Texas, United States of America.

Bijukchhen S, Takai N, Shigefuji M, Ichiyanagi M, Sasatani T, Sugimura Y (2017). Estimation of 1-D velocity models beneath strong-motion observation sites in the Kathmandu Valley using strong-motion records from moderate sized earthquakes. *Earth, Planets and Space*, 69(1): Article 97.

Boore DM (2004). Estimating Vs(30) (or NEHRP Site Classes) from Shallow Velocity Models (Depths <30 m). *Bulletin of the Seismological Society of America*, 94(2): 591-597.

Brandenberg SJ, Ballana N, Shantz T (2010). Shear Wave Velocity as a Statistical Function of Standard Penetration Test Resistance and Vertical Effective Stress at Caltrans Bridge Sites. *PEER Report 2010/03*, Pacific Earthquake Engineering Research Centre, University of California, Berkeley, California, United States of America.

BSI (2015) BS 5930: 2015: Code of practice for ground investigations. *British Standards Institution*, London, United Kingdom.

Casagrande A (1947). Classification and identification of soils. *Proceedings of the American Society of Civil Engineers*, 73(6): 783-810.

Castellaro S, Mulargia F, Rossi PL (2008). Vs30: Proxy for Seismic Amplification? *Seismological Research Letters*, 79(4): 540-543.

CEN (European Committee for Standardization) (2004). Eurocode 8: Design of structures for earthquake resistance – Part 1: General rules, seismic actions and rules for buildings. Brussels, Belgium.

Di Capua G, Lanzo G, Pessina V, Peppoloni S, Scasserra G (2011). The recording stations of the Italian strong motion network: geological information and site classification. *Bulletin of Earthquake Engineering*, 9(6): 1779-1796.

Dikmen U (2009). Statistical correlations of shear wave velocity and penetration resistance for soils. *Journal of Geophysics and Engineering*, 6(1): 61-72.

Dill HG (2006). An Overview of Younger Kathmandu Lake, Nepal, during the Late Quaternary, with Special Reference to Ferruginous Structures in Carbonaceous Sediments. *International Geology Review*, 48(5): 383-409.

Fabbrocino S, Lanzano G, Forte G, Santucci de Magistris F, Fabbrocino G (2015). SPT blow count vs. shear wave velocity relationship in the structurally complex formations of Molise Region (Italy). *Engineering Geology*, 187: 84-97.

Foti S, Hollender F, Garofalo F, Albarello D, Asten M, Bard PY, Comina C, Cornou C, Cox B, Di Giulio G, Forbriger T, Hayashi K, Lunedei E, Martin A, Mercerat D, Ohrnberger M, Poggi V, Renailier F, Scilia D, Socco V (2017). Guidelines for the good practice of surface wave analysis: a product of the InterPACIFIC project. *Bulletin of Earthquake Engineering*, 1-54, https://doi.org/10.1007/s10518-017-0206-7.

Fujii R, Sakai H (2002). Paleoclimatic changes during the last 2.5 myr recorded in the Kathmandu Basin, Central Nepal Himalayas. *Journal of Asian Earth Sciences*, 20(3): 255-266.

Gallipoli MR, Mucciarelli M (2009) Comparison of Site Classification from V_{S30}, V_{S10}, and HVSR in Italy. *Bulletin of the Seismological Society of America*, 99(1): 340-351.

Gautam D (2017). Empirical correlation between uncorrected standard penetration resistance (N) and shear wave velocity (V_s) for Kathmandu Valley, Nepal. *Geomatics, Natural Hazards and Risk*, 8(2): 496-508.

Goda K, Kiyota T, Pokhrel RM, Chiaro G, Katagiri T, Sharma K, Wilkinson S (2015). The 2015 Gorkha Nepal earthquake: insights from earthquake damage survey. *Frontiers in Built Environment*, 1: Article 8.

Guillot S (1999). An overview of the metamorphic evolution in Central Nepal. *Journal of Asian Earth Sciences*, 17(5-6): 713-725.

Howard AK (1984). The Revised ASTM Standard on the Unified Classification System. *Geotechnical Testing Journal*, 7(4): 216-222.

Jafari MK, Shafiee A, Razmkhah A (2002). Dynamic properties of fine grained soils in south of Tehran. *Journal of Seismology and Earthquake Engineering*, 4(1): 25-35.

Lee VW, Trifunac MD (2010). Should average shear-wave velocity in the top 30m of soil be used to describe seismic amplification? *Soil Dynamics and Earthquake Engineering*, 30(11): 1250-1258.

Luzi L, Puglia R, Pacor F, Gallipoli MR, Bindi D, Mucciarelli M (2011). Proposal for a soil classification based on parameters alternative or complementary to $V_{S,30}$. *Bulletin of Earthquake Engineering*, 9(6): 1877-1898.

McKenna, F, Fenves, GL, Scott, MH (2000). Open system for earthquake engineering simulation. University of California, Berkeley, CA, United States of America.

Molnar S, Onwuemeka J, Adhikari S (2017). Rapid Post-Earthquake Microtremor Measurements for Site Amplification and Shear-wave Velocity Profiling in Kathmandu, Nepal. *Earthquake Spectra*, 33(S1): S55-S72.

Ohsumi T, Mikai Y, Fujitani H (2016). Investigation of Damage in and Around Kathmandu Valley Related to the 2015 Gorkha, Nepal Earthquake and Beyond. *Geotechnical and Geological Engineering*, 34(4): 1223-1245.

Ohta Y, Goto N (1978). Empirical shear wave velocity equations in terms of characteristic soil indexes. *Earthquake Engineering and Structural Dynamics*, 6(2): 167-187.

Park CB, Miller RD, Xia J (1999). Multichannel analysis of surface waves. *Geophysics*, 64(3): 800-808.

Paudyal YR, Yatabe R, Bhandary NP, Dahal RK (2013). Basement topography of the Kathmandu Basin using microtremor observation. *Journal of Asian Earth Sciences*, 62: 627-637.

Pitilakis K, Raptakis D, Lontzetidis KT, Vassilikou T, Jongmans D (1999). Geotechnical and geophysical description of Euro-Seistest, using field and laboratory tests and moderate strong motion recordings. *Journal of Earthquake Engineering*, 3(3): 381-409.

Piya BK (2004). Generation of a Geological database for the Liquefaction hazard assessment in Kathmandu valley, *M.Sc. Thesis*, International Institute for Geo-information Science and Earth Observation, Enschede, The Netherlands.

Pokhrel RM, Kuwano J, Tachibana S (2013). A kriging method of interpolation used to map liquefaction potential over alluvial ground. *Engineering Geology*, 152(1): 26-37.

Poovarodom N, Chamlagain D, Jirasakjamroonsri A, Warnitchai P (2017). Site characteristics of Kathmandu Valley from Array Microtremor Observations. *Earthquake Spectra*, 33(S1): S85-S93.

Sakai H, Fujii R, Kuwahara Y (2002). Changes in the depositional system of the Paleo-Kathmandu Lake caused by uplift of the Nepal Lesser Himalayas. *Journal of Asian Earth Sciences*, 20(3): 267-276.

Seed HB, Idriss IM (1969). Influence of soil conditions on ground motions during earthquakes. *Journal of the Soil Mechanics and Foundations Division (ASCE)*, 95(1): 99-138.

Shi J, Asimaki D (2017). From Stiffness to Strength: Formulation and Validation of a Hybrid Hyperbolic Nonlinear Soil Model for Site-Response Analyses. *Bulletin of the Seismological Society of America*, 107(3): 1336-1355.

Shrestha OM, Kolrala A, Karmacharya SL, Pradhananga UB, Pradhan PM, Karmacharya R (1998). Engineering and environmental geological map of the Kathmandu Valley, scale 1:50,000. Department of Mines and Geology, Lainchaur, Kathmandu, Nepal.

Stein ML (2012). Interpolation of spatial data: some theory for kriging. *Springer Science & Business Media*.

Stewart JP, Liu AH, Choi Y (2003). Amplification Factors for Spectral Acceleration in Tectonically Active Regions. *Bulletin of the Seismological Society of America*, 93(1): 332–352.

Stewart JP, Klimis N, Savvaidis A, Theodoulidis N, Zargli E, Athanasopoulos G, Pelekis P, Mylonakis G, Margaris B (2014). Compilation of a Local V_S Profile Database and Its Application for Inference of V_{S30} from Geologic-and Terrain-Based Proxies. *Bulletin of the Seismological Society of America*, 104(6): 2827-2841.

Tallett-Williams S, Gosh B, Wilkinson S, Fenton C, Burton P, Whitworth M, Datla S, Franco G, Trico A, Dejong H, Novellis V, White T, Lloyd T (2016). Site amplification in the Kathmandu Valley during the 2015 M7.6 Gorkha, Nepal earthquake. *Bulletin of Earthquake Engineering*, 14(12): 3301-3315.

Wair BR, DeJong JT, Shantz T (2012). Guidelines for Estimation of Shear Wave Velocity Profiles. *PEER Report 2012/08*, Pacific Earthquake Engineering Research Centre, University of California, Berkeley, California, United States of America.

Wald DJ, Worden CB, Quitoriano V, Pankow KL (2006). ShakeMap® Manual, technical manual, users guide, and software guide, available at: http://pubs.usgs.gov/tm/2005/12A01/pdf/508TM12-A1.pdf (accessed 03/03/2018).

Wald DJ, Allen TI (2007). Topographic Slope as a Proxy for Seismic Site Conditions and Amplification. *Bulletin of the Seismological Society of America*, 97(5): 1379-1395.